Journal of Physics: Conference Series

Effect of Zn on corrosion behaviour of biodegradable Mg-Zn-Mn alloys evaluated by FE prediction and *in-vitro* testing

Effect of Zn on corrosion behaviour of biodegradable Mg-Zn-Mn alloys evaluated by FE prediction and *in-vitro* testing

X.Z. Lu [1, 2], L.C. Chan [2], X.J. Zou [1], C.P. Lai [2, a*]

[1]Hunan Provincial Key Laboratory of Intelligent Manufacturing Technology for High-performance Mechanical Equipment, Changsha University of Science and Technology, Changsha, 410114, China

[2]Department of Industrial and Systems Engineering, The Hong Kong Polytechnic University, Hung Hom, Kowloon, Hong Kong S.A.R., China

[a*]email: cp.lai@polyu.edu.hk

Abstract. Mg-Zn-Mn (ZM) alloy shows great potential in biomedical applications due to its biocompatibility and bio-essential element composition, as well as its favourable mechanical and degradation properties. This paper aims to explore the effect of Zn on corrosion behaviour of ZM alloys via finite element (FE) prediction and *in-vitro* testing. Microstructure analysis showed that Zn had the grain refinement effect, and the second phase of Mg-Zn between grains increased with the increase of Zn content, which improved the mechanical properties of the alloy significantly at the cost of acceptable reduction in plasticity. After a continuum damage mechanics (CDM)-based degradation model was applied to the FE package, the corrosion process of the ZM alloys was predicted. The results indicated that the grain boundary had poor corrosion resistance while the second phase facilitated delaying corrosion expansion. Furthermore, *in-vitro* tests were carried out and consistent results were obtained, i.e., the grain refinement made the entire corrosion process more uniform and severe corrosion in local areas was avoided, and the intergranular second phase was beneficial to delay the corrosion process. This study suggested that Mg-Zn-Mn alloy has satisfactory mechanical strength and controllable corrosion rate, which should be a promising candidate for future biomedical applications.

1. Introduction

Magnesium (Mg) alloys possess the advantages of light weight, high specific strength, good biocompatibility and degradability, their application in degradable medical implants has attracted much attention [1]. However, high corrosion rate is currently a major problem faced by Mg alloys as implants. Alloying has proven to be an effective method to enhance the corrosion resistance and mechanical properties of Mg alloys [2]. Biocompatibility and bio-essential elements, such as Zinc (Zn) and Manganese (Mn), would be the preferred choice. Zn has the remarkable strengthening effect on Mg alloy and thus improve the mechanical properties. Meanwhile, the corrosion process of Mg alloy can be delayed by the formation of a protective zinc phosphate layer during immersion [3,4]. Mn has the grain refinement effect and it can improve the yield strength of Mg alloy slightly. Moreover, the corrosion resistance of Mg alloy can be enhanced by reducing impurities and heavy-metal elements with a small quantity of Mn addition [5]. Therefore, alloying elements Zn and Mn were selected in this study to improve both the mechanical property and corrosion resistance of Mg alloys.

Finite element method (FEM) is believed to be a promising tool for the degradation prediction of biomaterials, particularly for Mg alloys [6]. Certain appropriate physical or phenomenological degradation models have been implemented into the finite element (FE) code for the degradation prediction [7]. Owing to the advantages of easier parameters determination and lower computational cost compared to the physical ones, the phenomenological continuum damage mechanics (CDM) based model is being used widely nowadays. This model has been proved to be an effective approach for modelling various biodegradation processes inside animal/living tissues with complex structures and complicated geometry [8]. Therefore, an improved CDM-based model considering micro-galvanic degradation and anisotropic plasticity under load-bearing conditions is adopted in this study.

Therefore, the main objective of this study is to explore the effect of Zn on corrosion behaviour of biodegradable Mg-Zn-Mn (ZM) alloys via FE prediction and *in-vitro* testing. Extruded ZM alloys with different contents of Zn were prepared as the specimen materials, compression tests were carried out to obtain the mechanical properties for strength evaluation and FE simulations. Microstructure was characterized and the CDM-based degradation model was employed for degradation prediction. Finally, *in-vitro* immersion tests were performed for the verification of FE predictions.

2. Materials and Methods

2.1. Materials preparation

The ZM alloy ingots have the nominal composition of Mg-0.5Mn with different contents of Zn (1.0, 2.0 and 3.0 wt.%) were prepared by melting pure Mg and Zn, Mg-10Mn (wt. %) master alloys in an electrical resistance furnace under the protection gases of CO_2 and Ar. Afterward, The ingots were homogenization treated at 340 °C for 24 h, cylindrical bars with diameter of 100 mm were then machined from the homogenized ingot and preheated to 350 °C for extrusion at the designated speed of 1 mm/s in a single pass. Finally, extruded Mg–*x*Zn–0.5Mn (*x*=1, 2, 3) alloy bars with diameter of 10 mm, hereinafter donated as ZM1, ZM2 and ZM3 respectively, were obtained.

2.2. Mechanical testing

Compression specimens with the dimension of Ø10 mm× 15 mm were cut from the extruded alloy bars. CMT5105GL Testing Machine was performed for compression testing at a displacement rate of 1.0 mm/min. At least three replicates were carried out for each testing. True stress-strain curves of the ZM alloys were obtained, then the mechanical properties, such as Young's modulus, yield stress and ultimate compressive stress, were acquired for strength evaluation and for subsequent FE simulations.

2.3. Microstructure characterization, immersion test and corrosion rate evaluation

Microstructure of the extruded ZM alloys was characterized by a scanning electron microscope (SEM, Phenom G2). Specimens were ground with SiC papers progressively down to 1600 grit and polished with diamond pastes, followed by etching in a solution of 5% Nitric acid for 20~25 s to reveal the microstructures of Mg matrix, grain boundary and second phases.

Specimens with the dimension of Ø10 mm× 4 mm cut from the extruded ZM alloys were used for *in-vitro* immersion tests. All specimens were ground, polished, cleaned in ethanol under the stimulation of ultrasonic for 5 minutes, then dried by air blower. Immersion tests were conducted at a physiological temperature of 36.5 ± 1 °C controlled by water bath in simulated body fluid (SBF) solution for 2 days. After immersion, the specimens were ultrasonically cleaned in ethanol and dried in open air. Then the surface morphologies contain corrosion products were observed by the SEM. Each test was repeated three times to ensure the reliability of the results.

In addition, the corroded specimens were further cleaned by chromate bath consisting of 200 g/L CrO_3 and 10 g/L $AgNO_3$ to remove corrosion products, and then cleaned with alcohol and dried. Then the corrosion rate (*CR*) was evaluated by mass loss using the following equation:

$$CR = (K \times \Delta\omega)/(A \times T \times D) \quad (1)$$

where K is a constant value of 87600, $\Delta\omega$ is the mass loss (g), A is the initial exposed surface area (cm^2), T is the immersion time (h), and D is the density of the tested alloy (g/cm^2).

2.4. CDM-based model for degradation prediction

In this study, a CDM-based model which considers not only micro-galvanic degradation but also stress degradation was implemented into FE package ABAQUS for the degradation prediction of ZM alloys under load-bearing conditions [3,8]. The CDM-based model introduces a damage variable D to indicate the degree of weakening in the mechanical properties due to corrosion. An effective stress tensor $\tilde{\boldsymbol{\sigma}}$ is introduced. The D is composed of micro-galvanic degradation D_M and stress degradation D_S, and given as

$$D=D_M+D_S \tag{2}$$

Wherein the evolution law of micro-galvanic degradation can be formulated as

$$\dot{D}_M=k_M\delta_M/L_e \tag{3}$$

where k_M is the kinetic parameter of the degradation process, δ_M is the material characteristic dimension and L_e is the FE mesh characteristic length.

In addition, the evolution law of stress degradation can be expressed as

$$\dot{D}_S=(L_e/\delta_S)(S\sigma_{eq}^{*}/(1-D))^R \text{ if } \sigma_{eq}^{*}\geq\sigma_{th}>0 \tag{4}$$

$$\dot{D}_S=0 \text{ when } \sigma_{eq}^{*}<\sigma_{th} \tag{5}$$

where σ_{eq}^{*} is the effective stress and σ_{th} denotes the threshold value of the critical effective stress. S and R are material constants related to the kinetics of the stress degradation; δ_S is a characteristic dimension of the stress degradation process.

The above CDM-based degradation model was then compiled and embedded into ABAQUS. Microstructural configurations, including the Mg matrix, grain boundary and second phase that depicted from SEM were served as the geometrical models in the FE package. Kinetic parameters and characteristic dimensions obtained through *in-vitro* tests, as well as the material constants that acquired from the compression tests were employed in the CDM-based degradation model. Details about the simulation procedure can refer to our published work [3].

3. Results & Discussion

3.1. Microstructure and mechanical properties

Fig. 1 demonstrated the SEM microstructure of the extruded ZM alloys. Owning to the extrusion process and the grain refinement of Zn element, the grain size of the extruded alloys decreased markedly, and the grain size was further refined with the increasing of Zn content, e.g., 30-35 μm at 1 wt.% Zn and 15-20 μm at 3 wt.% Zn. In addition, the grain size in ZM1 varied greatly and only a small amount of particulate phase was precipitated in the matrix; while with the increase of Zn content, a large number of particulate phases were precipitated along the grain boundary. EDS result confirmed that the particulate phase was Mg-Zn phase.

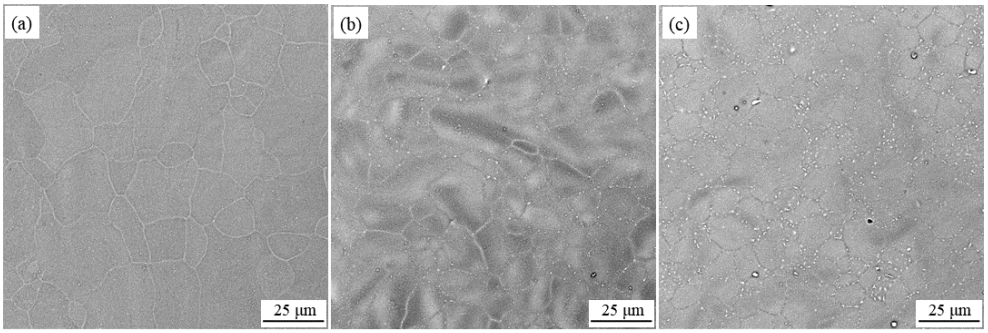

Fig. 1. Microstructure of the extruded ZM alloys: (a) ZM1, (b) ZM2 and (c) ZM3.

True stress-strains curves of the ZM alloys obtained from compression tests are shown in Fig. 2. It can be seen that the strength of the alloy increased significantly with the increasing of Zn content, i.e., the yield and compressive strengths were increased from 80.5 MPa and 333.8 MPa to 155.6 MPa and 402.5 MPa respectively with the Zn content increased from 1% to 3% (at. %). The increase of strength is attributed to the grain refinement effect and the intergranular second phase strengthening. Meanwhile, an acceptable reduction in plasticity was achieved, i.e., 0.236 for ZM1 and 0.197 for ZM3.

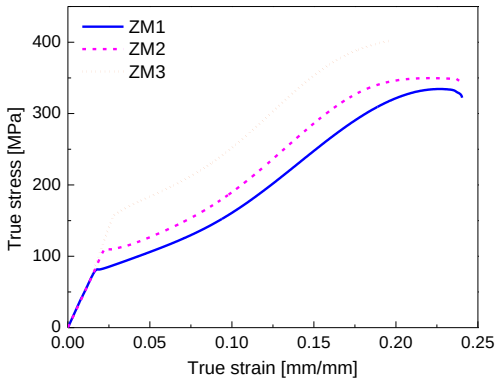

Fig. 2. True stress-strain curves of ZM alloys under compression.

3.2. Degradation prediction and verification

As described in Section 2.4, microstructural configurations of ZM alloys that depicted from SEM were employed as the geometrical FE models for degradation prediction. As shown in Fig. 3, unit cell with a side length of 30 μm is constructed, in which the Mg matrix, grain boundary and second phase are included, representing in yellow, red and blue respectively. The predicted results are shown in Fig. 4, and it can be seen that the grain boundary had poor corrosion resistance during the entire corrosion process, while the matrix and second phase were the opposite. Even in the early stage of corrosion, most of the grain boundaries were corroded for all the 3 specimens. Then the corrosion gradually expanded to the matrix along the grain boundary, while the second phase played a role in blocking/delaying the corrosion expansion. Therefore, for ZM1, in which basically no second phase existed, the matrix had obvious corrosion in the middle stage of corrosion; for ZM2 and ZM3, only partial of the matrix was corroded around the grain boundary. With the continuous erosion of the SBF (e.g., t=1.0), most of the surface area of ZM1 had obvious corrosion, and most of the matrix of ZM2 and ZM3 was corroded and only the second phase itself had not been corroded. In general, ZM2 and ZM3 possessed the better corrosion resistance than ZM1.

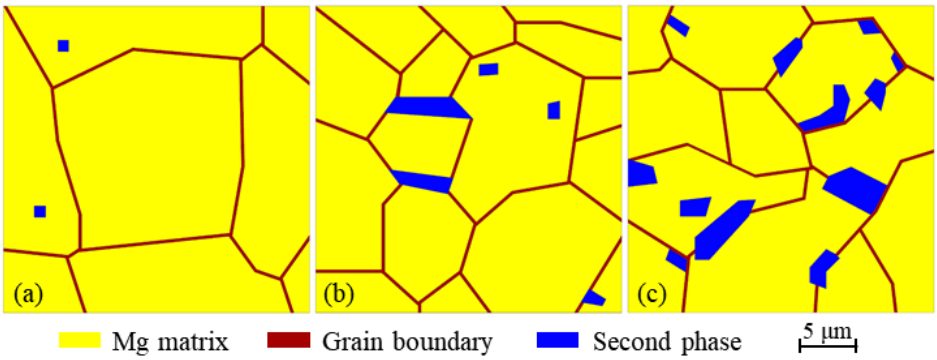

Fig. 3. FE models for degradation prediction of ZM alloys: (a) ZM1, (b) ZM2 and (c) ZM3.

Furthermore, *in-vitro* immersion tests were carried out for verification. Fig. 5 shows the corrosion morphologies of ZM alloys after 2 days immersion in SBF. It can be found that many trench-like corrosion paths appeared on the surface after washing and air-drying the soaked specimens. ZM2 and ZM3 had the uniform corrosion performance, while ZM1 had obvious local corrosion with some small pieces of flaking. Although the grain boundary corrosion effect was intensified due to smaller grain size introduced more grain boundaries, the grain refinement made the entire corrosion process more uniform and severe corrosion in local areas was avoided. Meanwhile, the increase in Zn content introduced more intergranular second phase of Mg-Zn, which was beneficial to the delay of corrosion process. The corrosion rate shown in Fig. 6 also confirmed that the ZM2 and ZM3 had the better corrosion resistant than that of ZM1. These testing results were consistent with the previous FE predictions, thus well verifying the validity of the proposed CDM-based degradation model.

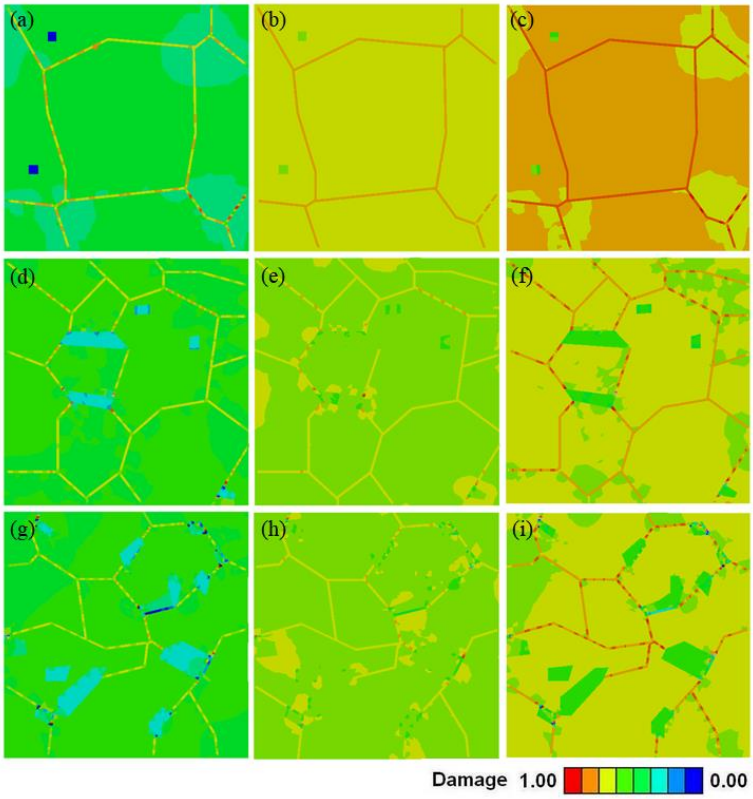

Fig. 4. Degradation prediction of ZM alloys: (a-c) ZM1 at t=0.1, 0.5 and 1.0 respectively; (d-f) ZM2 at t=0.1, 0.5 and 1.0 respectively; (g-i) ZM3 at t=0.1, 0.5 and 1.0 respectively.

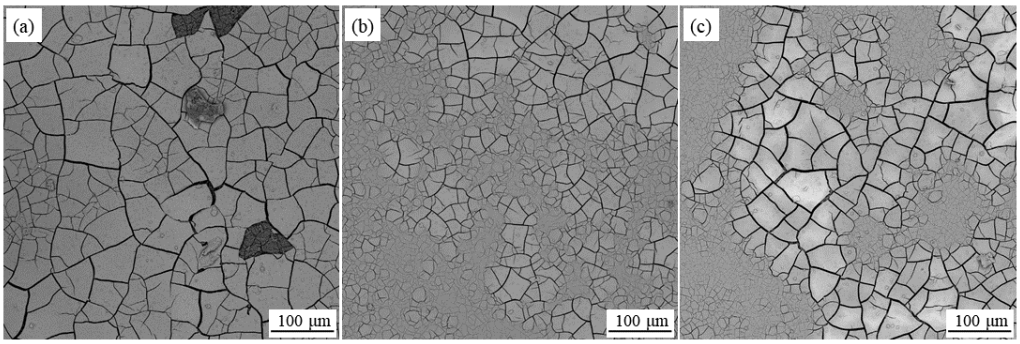

Fig. 5. Corrosion morphology of (a) ZM1, (b) ZM2 and (c) ZM3 alloys after 2 days immersion in SBF.

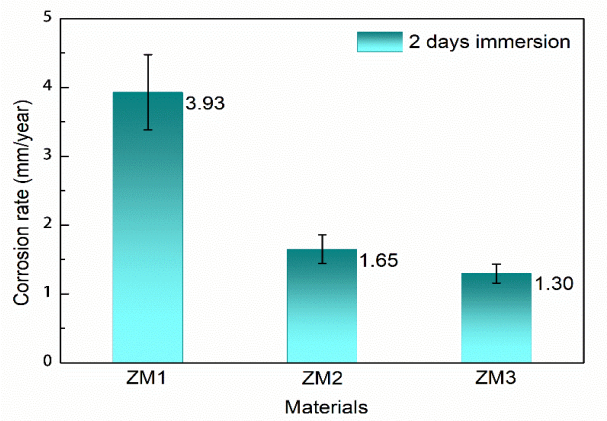

Fig. 6. Corrosion rates of ZM alloys after 2 days immersion in SBF.

4. Conclusions

(1) Zn has the grain refinement effect, and the second phase of intergranular Mg-Zn increased with the increase of Zn content, which improved the mechanical properties of the alloy significantly at the cost of acceptable reduction in plasticity.

(2) FE predictions showed that the grain boundary had poor corrosion resistance while the second phase facilitated delaying corrosion expansion, consistent results were obtained from the *in-vitro* tests. Therefore, the proposed CDM-based model is valid for the degradation prediction of ZM alloys.

(3) This study suggested that Mg-Zn-Mn alloy has satisfactory mechanical strength and controllable corrosion rate, which should be a promising candidate for future biomedical applications.

Acknowledgments

The work described in this paper was partially supported by Research Institute for Advanced Manufacturing of The Hong Kong Polytechnic University, general project of Education Department of Hunan Province (No. 19C0078) and Changsha Municipal Natural Science Foundation (No. kq2014095).

References

[1] Song, J.F., She, J., Chen, D.L., Pan, F.S. (2020) Latest research advances on magnesium and magnesium alloys worldwide. J. Magnes. Alloy., 8: 1-41.

[2] Ding, Y., Wen, C., Hodgson, P., Li, Y. (2014). Effects of alloying elements on the corrosion behavior and biocompatibility of biodegradable magnesium alloys: a review. J. Mater. Chem. B, 2: 1912-1933.

[3] Lu, X.Z., Lai, C.P., Chan, L.C. (2020) Novel design of a coral-like open-cell porous degradable magnesium implant for orthopaedic application. Mater. Des., 188: 108474.

[4] He, R., Liu, R., Chen, Q., Zhang, H., Wang, J., Guo, S. (2018) In vitro degradation behavior and cytocompatibility of Mg-6Zn-Mn alloy. Mater. Lett., 228: 77-80.
[5] Zhang, E., Yin, D., Xu, L., Yang, L., Yang, K. (2009) Microstructure, mechanical and corrosion properties and biocompatibility of Mg–Zn–Mn alloys for biomedical application. Mater. Sci. Eng. C, 29: 987-993.
[6] Shen, Z., Zhao, M., Bian, D., Shen, D., Zhou, X., Liu, J., Zheng, Y. (2019) Predicting the degradation behavior of magnesium alloys with a diffusion-based theoretical model and *in vitro* corrosion testing. J. Mater. Sci. Technol., 35: 1393-1402.
[7] Boland, E.L., Shine, R., Kelly, N., Sweeney, C.A., McHugh, P.E. (2016) A review of material degradation modelling for the analysis and design of bioabsorbable stents. Ann. Biomed. Eng., 44: 341-356.
[8] Wu, W., Chen, S.S., Gastaldi, D., Petrini, L., Mantovani, D., Yang, K., Tan, L.L., Migliavacca, F. (2013) Experimental data confirm numerical modeling of the degradation process of magnesium alloys stents. Acta Biomater., 9: 8730-8739.